

Three-dimensional numerical simulation of shock and detonation waves propagation in tubes with curved walls

Ilya Semenov^{†*}, Ildar Akhmedyanov^{*}, Alina Lebedeva^{*}, and Pavel Utkin^{*}

^{*}Institute for Computer Aided Design, Russian Academy of Sciences (ICAD RAS),
2nd Brestskaya, 19/18, Moscow 123056, RUSSIA
TEL : +7-499-2508286

[†]Corresponding address : semenov@icad.org.ru

Received : January 12, 2011 Accepted : March 9, 2011

Abstract

The mathematical model, the numerical method and the parallelization technique are presented for the problems of detonation initiation by means of comparatively weak shock wave and propagation of detonation waves in three-dimensional tubes of complex shapes. The mechanisms of detonation initiation in a tube with parabolic contraction and cone expansion and in a helical tube are analyzed. The results obtained are of interest both for basic research contributing to understanding of the mechanism of detonation initiation in tubes with curved walls and for applications from point of view of predictive modeling of accidents in chemical industry.

Keywords : numerical simulation, detonation initiation, parallel computations.

1. Introduction

It is known that propagation of even comparatively weak shock waves caused by energy releases into transport mains filled with reactive gaseous mixtures can produce detonation initiation and strong damages. Investigation of shocks propagation and possibility of detonation initiation in tubes with essential three-dimensional (3D) geometries is very important problem in the sense of operation safety of storage or transport environmental systems.

The 3D essence of gaseous detonation causes difficulties both in natural and numerical experiments. Existent studies of 3D detonations concern as a rule the structures of spinning¹⁾⁻³⁾ or multi-cellular detonation waves (DW) in straight round or square tubes^{4),5)}. One can mark out the following reasons preventing from extensive investigations of non-stationary transient regimes and effects of tube shape: (i) CPU time and memory costs for 3D problems, (ii) unstructured 3D grid generation for complex shapes, (iii) high-order numerical schemes construction for unstructured grids, (iv) effective parallelization of the numerical algorithm which deals with unstructured grids.

In our previous work shock-to-detonation transition (SDT) in 3D tube coils was investigated⁶⁾. The aim of the current work is to study the mechanism of SDT in tube with parabolic contraction and cone expansion and in helical tube which can be considered as the parts of transport mains systems.

2. Mathematical model

We use the system of equations that describe 3D unsteady flows of a reacting inviscid compressible multispecies gas mixture :

$$\frac{\partial q}{\partial t} + \frac{\partial f_1}{\partial x} + \frac{\partial f_2}{\partial y} + \frac{\partial f_3}{\partial z} = S \quad (1)$$

$$q = \begin{bmatrix} \rho_1 \\ \dots \\ \rho_N \\ \rho U_x \\ \rho U_y \\ \rho U_z \\ \rho E \end{bmatrix}, \quad f_1 = \begin{bmatrix} \rho_1 U_x \\ \dots \\ \rho_N U_x \\ \rho U_x^2 + p \\ \rho U_y U_x \\ \rho U_z U_x \\ (\rho E + p) U_x \end{bmatrix}, \quad f_2 = \begin{bmatrix} \rho_1 U_y \\ \dots \\ \rho_N U_y \\ \rho U_x U_y \\ \rho U_y^2 + p \\ \rho U_z U_y \\ (\rho E + p) U_y \end{bmatrix},$$

$$f_3 = \begin{bmatrix} \rho_1 U_z \\ \dots \\ \rho_N U_z \\ \rho U_x U_z \\ \rho U_y U_z \\ \rho U_z^2 + p \\ (\rho E + p) U_z \end{bmatrix}, S = \begin{bmatrix} \dot{\omega}_1 \\ \dots \\ \dot{\omega}_N \\ 0 \\ 0 \\ 0 \\ 0 \end{bmatrix}$$

Here t is the time; x, y, z are Cartesian coordinates; U_x, U_y, U_z are corresponding velocity components; ρ, p and E are the density, pressure, and total specific energy of the gas mixture; ρ_k and $\dot{\omega}_k$ are the density and density-variation rate due to chemical reactions of the k th species of the mixture. The total specific energy of the gas mixture is determined by the formula:

$$E = \frac{U_x^2 + U_y^2 + U_z^2}{2} + \sum_{k=1}^N \rho_k h_k / \rho - p / \rho \quad (2)$$

$$h_k = h_{0k} + c_{V_k} T + p_k / p_k / \rho_k, k = 1, \dots, N$$

where $p_k, h_k, h_{0k}, c_{V_k}$ are partial pressure, specific enthalpy, specific enthalpy of formation and specific heat at constant volume (which is considered to be constant) of the k th species of the mixture, N is the number of species in the mixture. Enthalpies of formation and specific heats were taken from⁷⁾.

The thermal equation of state of the mixture considered as a perfect gas is:

$$p = \sum_{k=1}^N p_k = \sum_{k=1}^N \rho_k \frac{R}{\mu_k} T \quad (3)$$

where T is the temperature, R is the universal gas constant, μ_k is molar mass of k th species.

The chemical reactions are modeled by one-stage kinetics of propane combustion⁸⁾:



Thus, the number of species N of the gas mixture considered is five. They are indexed in the following manner: C_3H_8 ($k = 1$), O_2 ($k = 2$), N_2 ($k = 3$), CO_2 ($k = 4$), H_2O ($k = 5$).

The density-variation rate for propane is determined as:

$$\omega_1 = \mu_1 \psi_1 = \mu_1 \left(k \frac{\rho_1}{\mu_1} \cdot \frac{\rho_2}{\mu_2} \right) \quad (5)$$

$$k = -7 \cdot 10^8 p^{-0.2264} \exp\left(-\frac{E^*}{RT}\right) [m^3 \cdot mol^{-1} \cdot sec^{-1}]$$

$$E^* = 190.3 \cdot 10^3 [J \cdot mol^{-1}]$$

where ψ_1 is the rate of variation of the propane molar fraction, p [atm] is the pressure, T [K] is the temperature. The density-variation rates for the remaining species of the mixture are determined via ψ_1 and the stoichiometric coefficients in reaction as:

$$\omega_2 = 5\mu_2\psi_1, \omega_3 = 0, \omega_4 = -3\mu_4\psi_1, \omega_5 = -4\mu_5\psi_1 \quad (6)$$

It should be noted that in spite of apparent simplicity one-stage kinetic models of chemical reactions are widely

used at present for investigations of multidimensional flows with DWs⁸⁾⁻¹⁰⁾.

3. Numerical procedure and parallelization technique

Method of splitting with respect to physical processes is used for the numerical solution of the problem. The system of gas dynamics equations is solved at first on the n th time step in the i th computational cell without right-hand source term S . The obtained solution $q_i^{gas, n+1}$ is updated then taking into account the source terms connected with chemical reactions.

The system of gas-dynamic equations is discretized with respect to spatial variables by means of the finite-volume method. The primary advantages of finite-volume methods are numerical robustness, applicability to general unstructured grids, and intrinsic local conservation properties of the resulting scheme¹¹⁾. To enhance the accuracy the MUSCL approach is used with upwind-biased third order (on uniform grids for one dimensional problems) scheme of interpolation of values at cell centers to faces¹²⁾. Vector of interpolated values to the face σ is denoted as $\tilde{q}_{i,\sigma}^n$. The gradient ∇q_i^n of the solution vector q_i^n is computed with the moving least squares method¹³⁾. Integration over time is performed by the explicit predictor-corrector scheme with the second-order approximation. The fluxes through the computational cells faces are calculated with Godunov's method.

The predictor stage can be written in the following manner:

$$\tilde{q}_i^{n+1} = q_i^n - \frac{\Delta t}{2V_i} \sum_{\sigma} \tilde{F}_{i,\sigma}^n \cdot s_{i,\sigma}, \tilde{F}_{i,\sigma}^n = T_{\sigma}^{-1} f_{i,\sigma}^n, f_{i,\sigma}^n = f_1(Q_{i,\sigma}^n) \quad (7)$$

$$Q_{i,\sigma}^n = T_{\sigma} q_{i,\sigma}^n$$

where V_i is the current cell volume, Δt is the time integration step, the summation is conducted over all faces σ of the cell i , $s_{i,\sigma}$ is the area of the corresponding face, $\tilde{F}_{i,\sigma}^n$ is the flux through the face σ , T_{σ} is the matrix of transformation from the laboratory frame of reference to the local one with one unit vector directed along outer normal and two others situated in the face σ .

The predictor stage is followed by the corrector stage that can be written as:

$$q_i^{gas, n+1} = q_i^n - \frac{\Delta t}{V_i} \sum_{\sigma} F_{i,\sigma}^n \cdot s_{i,\sigma}, F_{i,\sigma}^n = T_{\sigma}^{-1} \tilde{f}_{i,\sigma}^{n+1}, \tilde{f}_{i,\sigma}^{n+1} = f_1(\tilde{Q}_{i,\sigma}^{n+1}) \quad (8)$$

where $\tilde{Q}_{i,\sigma}^{n+1}$ is the exact solution of the Riemann's problem, corresponding to the initial data $\tilde{q}_{i,\sigma}^{n+1}$ and $\tilde{q}_{j,\sigma}^{n+1}$ on different sides of the discontinuity determined by the face σ . Here $\tilde{q}_{i,\sigma}^{n+1}$ stands for interpolated values vector \tilde{q}_i^{n+1} computed at predictor stage and then interpolated to the face σ with the use of gradient vector ∇q_i^n , index j corresponds to the values in the adjacent cell.

At the final stage the right-hand source terms connected with chemical reactions are taken into account by solving the corresponding system of ordinary differential equations with the use of backward

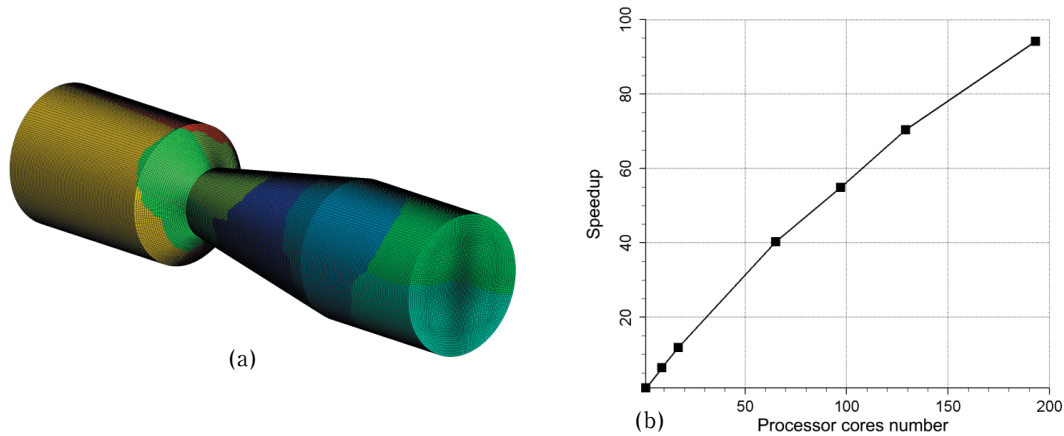


Fig. 1 The features of numerical algorithm parallelization: (a) the example of O-grid mesh used in calculations and its METIS decomposition into 10 parts; (b) the diagram of parallelization quality.

differentiation formulas.

The numerical algorithm is adapted for investigations to be performed on advanced multiprocessor computational systems with teraflop performance. Parallelization is performed by means of 3D decomposition of a computational domain. In our calculations we use unstructured grids with hexahedral cells which in the general case can be arbitrary associations of convex hexahedrons which can meet at faces, edges or vertexes. This fact causes certain difficulties in the implementation of the domain decomposition since cells which are close to each other geometrically can be strongly spread topologically and in the sense of the memory organization for grid storing. For domain decomposition implementation the open source package METIS for graphs partitioning is used¹⁴. It is worth noticing that METIS is widely used in commercial CFD packages such as ANSYS for the domain decomposition.

The example of O-grid used in calculations for detonation initiation in tubes with parabolic contraction and cone expansion and its partitioning with METIS on $K = 10$ parts is shown at Fig. 1a. Let us consider the quantitative characteristics of the quality of grid partitioning with METIS. The size of the test grid on Fig. 1 is 2,929,360 cells, the total number of faces is 8,734,740. After partitioning the deviation of the cells number in each part from the value $2,929,360 / K$ does not exceed 2%. At the same time the total number of faces on which the cells from different parts border is 98,693. Let us estimate the minimum number of faces on which the cells from different parts border in case of one-dimensional decomposition and structured grid. The cells number in the cross section approximately equals 10,000 and so the number of boundary cells in case of partitioning into 10 parts is approximately 90,000. We can see that the actual number of boundary cells differs from the estimated minimum for the one-dimensional decomposition by less than 10%.

We use from 200 to 600 processor cores for calculations on multiprocessor systems MVS-100 k (Joint Supercomputer Center RAS) or SKIF MSU. The characteristic spatial resolution of the processes in question is about 0.3mm, time resolution is from 5 to 10 ns.

The speedup (the ratio of the time it takes to execute a calculation on one core to the it takes to execute the same calculation on N cores) for the test problem solution on the grid with about 9 million. cells versus processor cores number is demonstrated on Fig. 1b. It is worth noticing that the speedup is 94 if we use 190 processor cores and effectiveness (the ratio of the speedup to the processor cores number) is about 50% and it is considered to be good enough in the sense of reasonable use of computational resources.

4. Verification

The mathematical model and the numerical procedure realized in the software for detonation initiation modeling were verified against several test problems.

The model of the chemical reactions kinetics was verified by experimental data on self-ignition delays measurements in shock tubes¹⁵. The comparison of experimental and calculated in case of one-dimensional studies self-ignition delays in shock tube indicates reasonable agreement (see Fig. 2a).

Another typical test case is the modeling of two-dimensional DW structure. Detonation was initiated by means of energy release near the closed end of a plane channel at $X=0$. The spatial resolution of the grid is 0.01 mm. A typical snapshot of a developed detonation front is shown in Fig. 2b. The resulting cellular patterns are very irregular and contain several levels of detonation cells, as one would expect for highly unstable detonation of stoichiometric propane-air mixture. One half of large cell occupies the whole channel so the calculated detonation cell width is about 10 mm which is an order of magnitude of experimental value 35 mm¹⁶.

5. Shock-to-detonation transition in a tube with parabolic contraction and cone expansion

Earlier the mechanism of detonation initiation in a tube with parabolic contraction and cone expansion was revealed on the basis of numerical experiment in axisymmetric statement¹⁷ and also the "optimal" shape of parabolic contraction was found which provides detonation initiation for initiating shock wave (SW) Mach

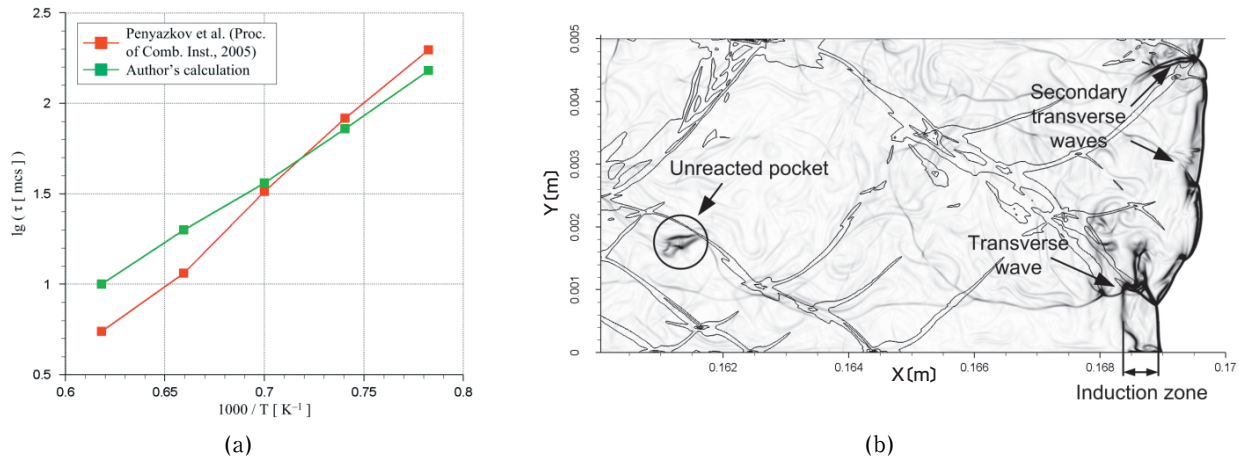


Fig. 2 Results of verification test cases: (a) the comparison of measured and calculated self-ignition delays in stoichiometric propane-air mixture (density behind reflected SW is $4.42 \text{ [kg} \cdot \text{m}^{-3}]$); (b) the structure of two-dimensional DW front, numerical Schlieren visualization and isolines of maximum pressure.

number 2.65 for the blockage ratio 0.75. The stoichiometric propane-air mixture is used as a reactive medium. Subsequently the results of these calculations were confirmed in experiments¹⁸. It was shown experimentally that for the “optimal” shape of parabolic contraction and angle of cone expansion 20° there exists a critical initiating SW Mach number 2.85. If the initiating SW Mach number exceeds the critical value SDT occurs and SDT doesn't occur in the opposite case. In experimental investigation¹⁹ the length of the divergent cone segment was substantially increased to optimize the process of detonation initiation. In this case the critical initiating SW Mach number was reduced to value 2.0.

Current work aims to investigate the process of SDT in the tube with parabolic contraction and cone expansion in 3D statement.

We consider an axisymmetric round tube which consists of a constant-section segment (1), a segment with parabolic contraction and cone expansion (2) and a constant-section outlet segment (3). Initially the tube is filled with a quiescent stoichiometric propane-air mixture under normal conditions. The parabolic profile of segment 2 is described by the curve $z(r)$. The quadratic dependence $z(r)$ is constructed to obtain a specified blockage ratio of the tube $BR = 1 - (d/D)^2$ and a specified angle ϕ of inclination of the profiled segment; the focus of the resultant parabola lies on the symmetry axis of the tube. For the investigation the “optimal” shape of contraction with $\phi = 45^\circ$, $BR = 0.75$ ¹⁷ was chosen. The motion of gas mixture in the tube is assumed to be initiated by a SW with zero gradients of parameters directly behind the SW with the Mach number M .

In computations the hexahedral grids with about 20 mln. cells were used.

The results of 3D numerical study in whole confirm basic stages and special features of the detonation initiation mechanism in the same tube revealed in axisymmetric calculations in¹⁷. Fig. 4 illustrates the results of 3D numerical modeling for the case $\phi = 45^\circ$, $BR = 0.75$, $M = 2.8$. For the purpose of 3D visualization of the processes under consideration, we use isosurfaces of

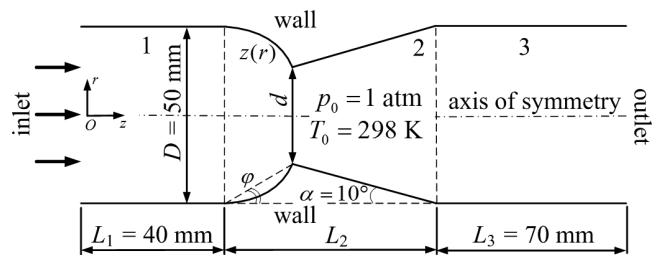


Fig. 3 Sketch of a tube with parabolic contraction and cone expansion.

pressure and propane density, and also pressure and temperature fields over the tube longitudinal section and over indicated isosurfaces. The isovalues in each particular case are chosen for the most evident visualization of the initiation stage under consideration. The time is counted from the moment when the initiating SW enters the tube.

It is possible to single out three basic stages of the initiation process. At the first stage, we observe the double Mach reflection of the leading SW from the parabolic contraction (see Fig. 4a). The second stage is the formation of one or two local explosions connected with Mach wave or reflected SW cumulation on the symmetry axis of the tube (see Fig. 4b). The third stage is detonation reinitiation due to the reflection of a blast wave caused by the local explosion from the walls of the cone expansion (see Fig. 4c). The value of angle α is an important parameter, and it was substantially reduced in¹⁹ to optimize the reinitiation stage. After detonation reinitiation and the by-pass of DW into segment 3 we observed the typical 3D pattern (see Fig. 4d), which is detected in numerous experiments on the DW front structure in the tube outlet cross section.

6. Shock-to-detonation transition in a helical tube

The next series of numerical experiments we investigated concern a tube of a constant round cross section with the diameter 28mm consisted of an inlet segment S_1 , a helical segment S_2 and an outlet segment S_3 (see Fig. 5). The helical segment S_2 in turn consists of three parts. The first part S_2^1 is a surface, swept by a circle during its motion divided into three components: uniform

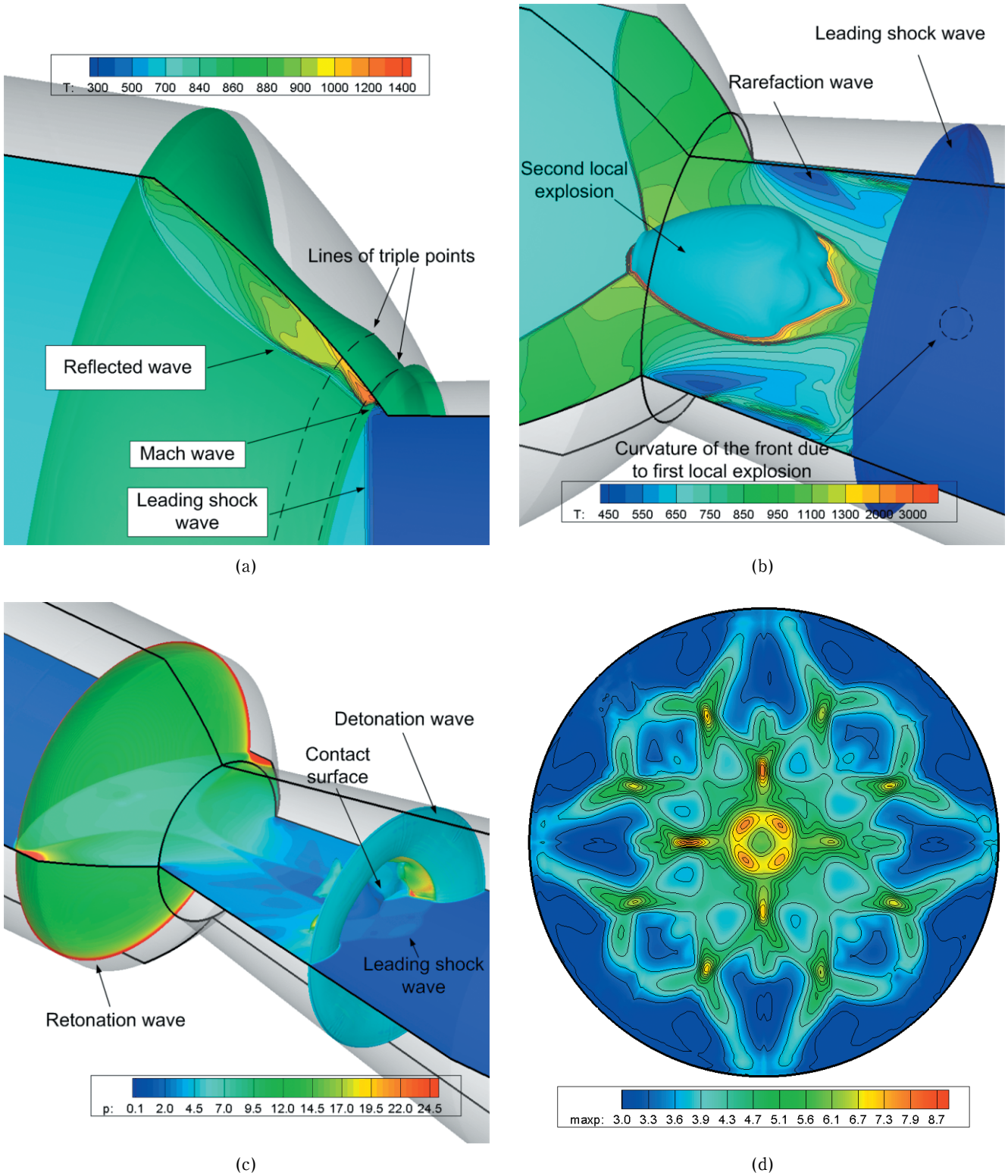


Fig. 4 Detonation initiation mechanism : (a) the pressure isosurface of 16 atm and the temperature field over the longitudinal section at $60 \mu s$; (b) the pressure isosurface of 1.1 atm and the propane mass fraction of 0.055, and the temperature field over the longitudinal section at $80 \mu s$; (c) the propane density isosurface of $0.05 \text{ kg} \cdot \text{m}^{-3}$ with the pressure field over it and the pressure field over the longitudinal section at $95 \mu s$; (d) “numerical soot footprint” in the outlet segment of the tube at $135 \mu s$.

motion along the X axis, uniform rotation about 90° around the X axis and circle center’s uniform movement away from the X axis. The second part S_2^2 is a cylindrical helical surface of one complete turn round the X axis. The third part S_3^2 is analogous to the first one, except that the circle center doesn’t move away from the X axis, but goes back to it. So it could be said that the tube’s surface is

created by sweeping the circle positioned in YZ plane with its center uniformly moving along a curve represented by equation :

$$x = 28 \cdot m, y = \begin{cases} 28 \cdot m \cdot \cos(90^\circ \cdot m), & m \in [0;1] \\ 28 \cdot \cos(90^\circ \cdot m), & m \in [1;5] \\ 28 \cdot (6 - m) \cdot \cos(90^\circ \cdot m), & m \in [5;6] \end{cases}$$

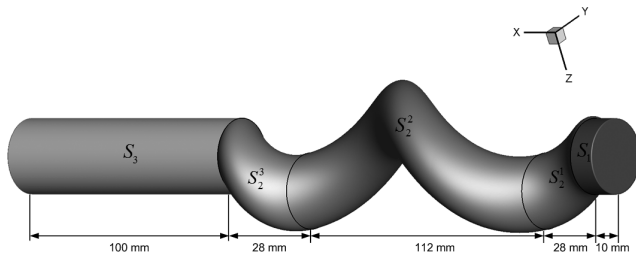


Fig. 5 The helical tube geometry.

$$z = \begin{cases} 28 \cdot m \cdot \sin(90^\circ \cdot m), & m \in [0;1] \\ 28 \cdot \sin(90^\circ \cdot m), & m \in [1;5], m \in [0;6] \\ 28 \cdot (6 - m) \cdot \sin(90^\circ \cdot m), & m \in [5;6] \end{cases} \quad (9)$$

In numerical experiments with the helical tube we used hexahedral multi-block O-grid meshes with about 5 and 30 million cells.

Let's consider numerical experiments over the mesh with 5 million cells. Initially a plane SW with Mach numbers $M = 3.4, 3.2$ or 3.0 enters the inlet segment S_1 orthogonally to the X axis, similarly to the previous problem definition. Our numerical experiments indicated detonation initiation throughout the cross section when initiating SW Mach number equaled 3.4. For $M = 3.2$ spinning detonation in outlet segment S_3 was observed. For $M = 3.0$, although there was a local explosion, detonation process decayed quickly and non-detonational combustion took place.

Due to the tube surface geometry initiating SW experiences Mach reflection from the wall, and we can see the triple point trace on the tube surface. Pressure and temperature go higher in vicinity of the triple point which makes conditions favorable for spontaneous ignition. Self-ignition near the wall occurs in all three numerical experiments. That source of ignition causes a blast wave that propagates through preheated media and interacts with the wall giving rise to the second source of self-ignition which occurs in numerical experiments for $M = 3.2$ and $M = 3.4$ (see Fig. 6). For $M = 3.0$ the intensity of the blast wave and the temperature of preheated media appears not enough to enable the second self-ignition. Due to fast growing volume of ignited mixture in experiments with $M = 3.4$ or 3.2 secondary SWs arise, therefore leading

SW front accelerates.

In the experiment with initiating SW with Mach number 3.4 after leading SW by-passes into outlet segment S_3 DW develops throughout the cross section with complicated DW front structure. For $M = 3.2$ after leading SW by-passes into outlet segment S_3 we can see spinning detonation (see Fig. 7). Numerous empirical studies have shown that the motion path of "spin head" on the tube surface is a helical curve inclined 45° with respect to generating lines of a tube²⁰. Experimentally such helical curves are detected by means of the soot foil technique. The tracks on sooted surfaces are associated with the triple point's motion paths. We used "numerical soot footprints" to capture "spin head" traces. In case of $M = 3.2$ "spin head" trace is inclined approximately 50° with respect to generating lines. It's worth noticing that in numerical experiment for $M = 3.2$ with more detailed mesh (almost 30 million cells) spinning mode was reproduced.

7. Conclusions

The paper presents the mathematical model, the numerical method and the parallelization technique for the problems of detonation initiation and propagation in 3D tubes of complex shapes. Also, quantitative characteristics of quality of parallelization based on computational domain 3D decomposition are presented.

The analysis of detonation initiation mechanism taking place in axisymmetric tube with parabolic contraction and cone expansion has been performed. The results of 3D numerical investigation of that tube in whole confirm basic stages and features of detonation initiation mechanism that have been revealed in axisymmetric computations¹⁷. However, 3D case indicated decay of initially axial symmetric flow structure associated with instability of DW front.

The mechanism of detonation initiation in the helical tube has been analyzed, and combustion modes have been classified. It appears that when initiating SW Mach exceeds some critical value the detonation throughout the outlet cross section is observed. Some weakening of initiating SW leads to spinning detonation. Further weakening of initiating SW results in non-detonational

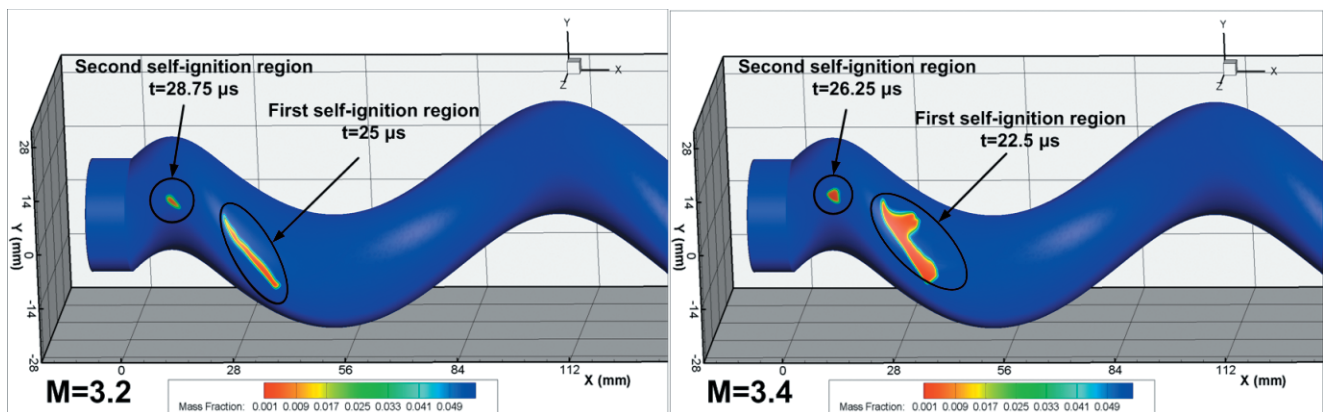


Fig. 6 Appearance of self-ignition regions for the cases of successful detonation initiation. Distributions of propane mass fraction over the tube surface.

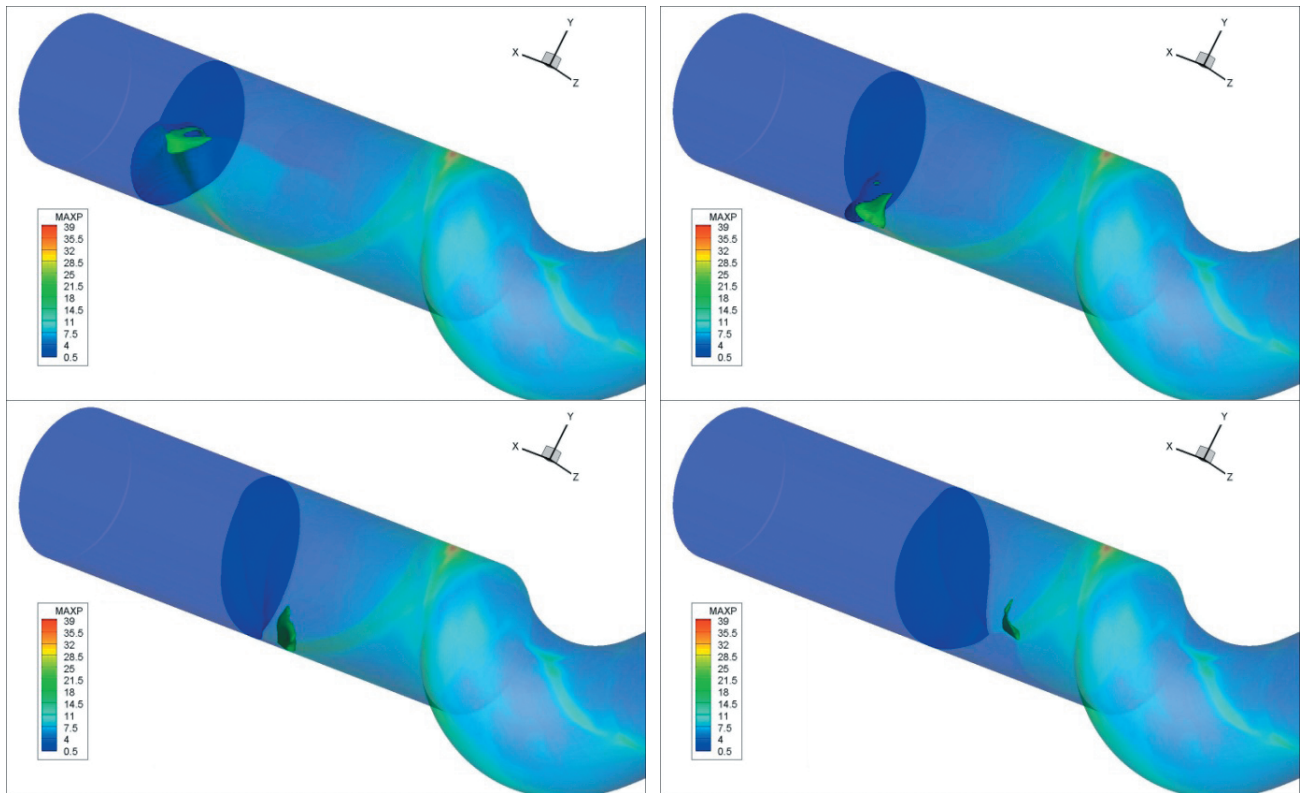


Fig. 7 Spinning detonation mode. “Numerical soot footprints”—distributions of pressure maximums in MPa.

combustion mode.

The results obtained are of interest for applications from point of view of predictive modeling of accidents in chemical industry.

Acknowledgments

This work was supported by Special Federal Program “Scientific and scientifically educational staff of innovation Russia” (NK-100P, contract №P-359).

References

- 1) N. Tsuboi, K. Eto and K. Hayashi, *Comb. Flame*, 149, 144 (2007).
- 2) F. Viot, M. Kurosaka, B. Khasainov, D. Desbordes and H. Presles, *Proc. Seventh International Symposium on Hazards, Prevention and Mitigation of Industrial Explosions*, Vol.2, pp. 66–72, St. Petersburg (2008).
- 3) A. Kobeira, M. Folusiak, K. Swiderski, J. Kindracki and P. Wolanski, *Proc. Twenty-Second International Colloquium on the Dynamics of Explosions and Reactive Systems*, paper 45 (2009).
- 4) V. Deledicque and M. Papalexandris, *Comb. Flame*, 144, 821 (2006).
- 5) H.-S. Dou, H. Tsai, B. Khoo and J. Qiu, *Comb. Flame*, 154, 644 (2008).
- 6) S. Frolov, I. Semenov, I. Ahmetyanov and V. Markov, *Proc. Twenty-Sixth International Symposium on Shock Waves*, Vol.1, pp. 365–370 (2009).
- 7) B. McBride, S. Gordon and M. Reno, NASA Report TM-4513, October 1993.
- 8) S. Frolov, V. Aksenov and I. Shamshin, “Nonequilibrium processes”, Vol.1, p. 348, Torus Press (2005).
- 9) E. Oran, V. Gamezo, *Comb. Flame*, 148, 4 (2007).
- 10) V. Levin, I. Manuilovich and V. Markov, *Doklady Physics*, 55, 28 (2010).
- 11) T. Barth and M. Ohlberger, “Finite Volume Methods: Foundation and Analysis”, In: “Encyclopedia of Computational Mechanics”, Vol.1, p. 437, Wiley (2004).
- 12) B. Van Leer, *J. Comput. Phys.*, 32, 101 (1979).
- 13) A. Gossler, Sandia Report SAND2001–1669, (2001).
- 14) G. Karypis G. and V. Kumar, “METIS 4.0: Unstructured Graph Partitioning and Sparse Matrix Ordering System”, Tech. report, Depart. Comp. Science, Univ. Minnesota, (1998).
- 15) O. Penyazkov, K. Ragotner, A. Dean and B. Varatharajan, *Proc. Comb. Inst.*, 30, 1941 (2005).
- 16) A. Vasil’ev, *Comb., Expl. and Shock Waves*, 44 (1), 86 (2008).
- 17) I. Semenov, P. Utkin and V. Markov, *Comb., Expl. and Shock Waves*, 45, 700 (2009).
- 18) I. Semenov, P. Utkin, V. Markov, S. Frolov and V. Aksenov, *Proc. Twenty-Second International Colloquium on the Dynamics of Explosions and Reactive Systems*, paper 168 (2009).
- 19) S. Frolov and V. Aksenov, *Doklady Physical Chemistry*, 427, 129 (2009).
- 20) V. Mitrofanov, “Detonation of Homogeneous and Heterogeneous Systems”, Novosibirsk: Publ. of the Inst. of Hydrodynamics after M.A. Lavrentyev SD RAS (2003).